
SPARSE AND LOW-RANK HIGH-ORDER TENSOR REGRESSION VIA PARALLEL PROXIMAL METHOD

A PREPRINT

Jiaqi Zhang

Department of Computer Science
Brown University

Yinghao Cai

Department of Computer Science
Southeast University

Zhaoyang Wang

Department of Computer Science
Southeast University

Beilun Wang*

Department of Computer Science
Southeast University

ABSTRACT

Recently, tensor data (or multidimensional array) have been generated in many modern applications, such as functional magnetic resonance imaging (fMRI) in neuroscience and videos in video analysis. Many efforts are made in recent years to predict the relationship between tensor features and univariate responses. However, previously proposed methods either lose structural information within tensor data or have prohibitively expensive time costs, especially for large-scale data with high-order structures. To address such problems, we propose the Sparse and Low-rank Tensor Regression (SLTR) model. Our model enforces sparsity and low-rankness of the tensor coefficient by directly applying ℓ_1 norm and tensor nuclear norm, such that it preserves structural information of the tensor. To make the solving procedure scalable and efficient, SLTR makes use of the proximal gradient method, which can be easily implemented parallelly. We evaluate SLTR on several simulated datasets and one video action recognition dataset. Experiment results show that, compared with previous models, SLTR can obtain a better solution with much fewer time costs. Moreover, our model's predictions exhibit meaningful interpretations on the video dataset.

1 Introduction

Tensor data, also called multidimensional array data, is frequently seen in various scientific and real-world applications, including neuroscience (Zhu et al., 2014; Noroozi and Rezghi, 2020), video analysis (Wu and Lai, 2010; Lui, 2012; Yang et al., 2017), and recommendation system design (Sharma and Gera, 2013; Bhargava et al., 2015). For example, functional magnetic resonance imaging (fMRI) data in neuroscience contains a series of 3D tensors (3-mode or 3-order data) with the shape of $time \times neuron \times neuron$. The researchers use such data to predict scalar-valued disease symptoms such as Mild Cognitive Impairment (Zhu et al., 2014). Many studies analyze the relationship between a tensor variable and its corresponding scalar response through the so-called *tensor regression* (Ji et al., 2019).

The emergence of tensor data enables researchers to analyze the system with the presence of structural correlations. However, the characteristics of tensor data also present new challenges for statistical analysis. First, the tensor data are usually high-dimensional, so the number of observations is much less than the number of variables. For example, each sample of the CMU2008 fMRI dataset (Mitchell et al., 2008) is a $51 \times 61 \times 23$ 3D tensor with 71553 voxels. But, only 360 samples are recorded. Conventional methods are mostly likely to fail in high-dimensional settings since we are trying to infer a large number of unknowns with limited observations. Second, tensor data have a high-order structure. For example, in the recommendation system, we need to predict recommendation levels from 4D user activities $user \times product \times location \times timestamp$ (Bhargava et al., 2015). Hence, existing linear regression models cannot be directly applied to tensors. Because such a method is designed for vector data and may lose the spatial structure of the data, like pixel relations in pictures or time orders in videos. Moreover, as the number of variables increases exponentially with

*To whom correspondence should be addressed.

the number of dimensions, higher-order data contains more unknown variables and requires significantly expensive computational costs.

To address these challenges, recent tensor regression methods adopt sparse and low-rank constraints from vector or matrix regression methods. The sparse constraint filter out "useless" variables, generally obtained through variable selection (Heinze et al., 2018), to decrease the number of variables. On the other hand, enforcing low-rank constraints reduces the complexity of the model that fits the data. These constraints make the tensor regression problem more tractable. For example, (Zhou et al., 2013; He et al., 2018) use CANDECOMP/PARAFAC (CP) decomposition to characterize an M -order tensor with multiple components and add structural constraints on each. However, all the CP decomposition-based methods suffer the drawbacks of slow convergence (Li et al., 2013) and inaccurate prediction since the best CP approximation might not exist (Cichocki et al., 2016).

Therefore, some methods directly apply structural constraints on tensors to avoid the decomposition (Song and Lu, 2017; Li et al., 2019) or use the more flexible Tuck decomposition (Ahmed et al., 2020). However, they are computationally expensive because of expensive procedures, including optimizing multiple nuclear norms. Due to their drawbacks, the above methods can not obtain a solution efficiently for large-scale tensor data. Therefore, we need a fast and scalable tensor regression estimator.

In this paper, we propose the Sparse and Low-Rank High-Order Tensor Regression (SLTR) method. Our model directly applies sparse and low-rank constraints through ℓ_1 norm and nuclear norm to decrease the model complexity of tensor regression. To speed up the optimization, we also propose a scalable solution, making use of the parallel proximal method (Combettes and Pesquet, 2011) that can be implemented parallelly. Therefore, through multi-threading computation or Graphics Processing Units (GPUs), the optimization of SLTR vastly reduces the computational time cost. We theoretically prove the sharp error bound of our model. Moreover, we compare our model with four state-of-the-art tensor regression methods on several simulated datasets and one video action recognition dataset (Soomro et al., 2012). Results show that our SLTR can obtain better solutions with much fewer time costs.

2 Notation

We let calligraphic characters denote an M -order tensor $\mathcal{A} \in \mathbb{R}^{p_1 \times \dots \times p_M}$ with the size of each dimension as $\mathcal{P} = \{p_1, \dots, p_M\}$. Uppercase characters A denote matrices and lowercase characters a denote vectors. $\|\cdot\|_1$ and $\|\cdot\|_\infty$ represent element-wise ℓ_1 norm element-wise ℓ_∞ norm correspondingly. Moreover, $\|\cdot\|_F$ is the element-wise ℓ_2 norm (Frobenius norm). For a matrix, $\|\cdot\|_2$ and $\|A\|_*$ denote the spectral norm and nuclear norm. We also use the same notations for nuclear and spectral norms of tensors. They can be distinguished based on context.

We introduce some basic operations for the tensor data. The inner product for two tensor $\mathcal{A}, \mathcal{B} \in \mathbb{R}^{p_1 \times \dots \times p_M}$ is the sum of products of every entries, defined as $\langle \mathcal{A}, \mathcal{B} \rangle = \sum_{i_1=1}^{p_1} \dots \sum_{i_M=1}^{p_M} \mathcal{A}_{i_1 \dots i_M} \mathcal{B}_{i_1 \dots i_M}$. The m -mode product of an M -order tensor \mathcal{A} by a matrix $A \in \mathbb{R}^{J \times p_m}$, denoted by $\mathcal{A} \times_m A$, is a tensor with the shape $\mathbb{R}^{p_1 \times \dots \times p_{m-1} \times J \times p_{m+1} \times \dots \times p_M}$. Here, each entry of the m -order product is given by $(\mathcal{A} \times_m A)_{i_1 \dots i_{m-1} j i_{m+1} \dots i_M} = \sum_{i_m=1}^{p_m} \mathcal{A}_{i_1 \dots i_M} a_{j i_m}$.

3 Background and Formal Problem Statement

3.1 Tensor Regression

In this paper, we consider modelling the relationship between M -order tensor variable $\mathcal{X}_i \in \mathbb{R}^{p_1 \times \dots \times p_M}$ and corresponding scalar response y_i from N observations ($i = 1, 2, \dots, N$). We assume a linear relationship as

$$y_i = \langle \mathcal{W}, \mathcal{X}_i \rangle + \gamma_i, \forall i = 1, \dots, N, \tag{1}$$

where $\langle \cdot, \cdot \rangle$ is the tensor inner product operator and $\gamma_i \in \mathbb{R}$ is the noise assumed to be drawn from a Normal distribution $\mathcal{N}(0, \alpha)$ with a relatively small α . The M -order coefficient tensor $\mathcal{W} \in \mathbb{R}^{p_1 \times \dots \times p_M}$ measures how each variable of \mathcal{X} contributes to the response. We estimate \mathcal{W} with tensor regression² that solves

$$\widehat{\mathcal{W}} = \arg \min_{\mathcal{W}} \sum_{i=1}^N (y_i - \langle \mathcal{W}, \mathcal{X}_i \rangle)^2. \tag{2}$$

²Based on the order of response, there are different types of tensor regression problems. For example, the tensor-on-tensor regression methods analyze tensor responses. In this paper, we focus on the tensor-on-scalar case where the response is a scalar value.

3.2 Regularized Tensor Regression

To reduce the model complexity, state-of-the-art tensor regression methods always add sparse or low-rank constraints on estimations and solve the regularized tensor regression

$$\widehat{\mathcal{W}} = \arg \min_{\mathcal{W}} \sum_{i=1}^N (y_i - \langle \mathcal{W}, \mathcal{X}_i \rangle)^2 + \mathcal{R}(\mathcal{W}) \quad (3)$$

with a regularization term $\mathcal{R}(\cdot) : \mathbb{R}^{p_1 \times \dots \times p_M} \mapsto \mathbb{R}$. Different regularizations lead to various structural properties.

Regularization for Sparsity Tensor data is usually high-dimensional. Therefore, to solve the ill-defined tensor regression problem, some tensor regression models (He et al., 2018; Zhou et al., 2013) adopt ideas from sparse linear regression. Specifically, they assume only a small subset of variables contribute to the response, so \mathcal{W} has many zero coefficients. They solve Eq. (3) with an element-wise ℓ_1 norm enforcing the coefficient sparsity as

$$\mathcal{R}_{\text{sparse}}(\mathcal{W}) = \|\mathcal{W}\|_1 = \sum_{i_1=1}^{p_1} \dots \sum_{i_M=1}^{p_M} |\mathcal{W}_{i_1 \dots i_M}|. \quad (4)$$

Our model uses the element-wise ℓ_1 norm to achieve prediction sparsity.

Regularization for Low-Rankness On the other hand, previous works (Song and Lu, 2017; Li et al., 2019; Zhou et al., 2013; He et al., 2018) also use low-rank constraints to reduce model complexity. But computing tensor rank is NP-hard (Shitov, 2016; Lim and Hillar, 2009). So they usually optimize with tensor decomposition to compute the best fitting rank in a tractable way (Rabanser et al., 2017). CP decomposition and Tucker decomposition are two widely used tensor decomposition techniques (Tucker, 1966; Rabanser et al., 2017). But CP decomposition methods suffer the drawbacks of slow convergence and inaccurate prediction. Compared to CP decomposition, Tucker decomposition is a direct extension of singular value decomposition (SVD), hence, it better cooperates with existing optimization algorithms. So in this paper, we use Tucker decomposition as

$$\mathcal{W} = \mathcal{C} \times_1 W_{(1)} \times_2 W_{(2)} \times_3 \dots \times_M W_{(M)} \quad (5)$$

where $\mathcal{C} \in \mathbb{R}^{p_1 \times \dots \times p_M}$ is the core tensor. Matrix $W_{(m)} \in \mathbb{R}^{p_m \times \prod_{k \neq m} p_k}$ is the result of unfolding the tensor \mathcal{W} along the m -th order. \times_m is the m -mode product operator defined in Section 2. The tensor \mathcal{W} is low-rank as long as $\{W_{(1)}, \dots, W_{(M)}\}$ are all low-rank.

But it is difficult to directly obtain the tensor rank through Eq. (5). Fortunately, as proven in Tomioka et al. (2010); Liu et al. (2012), we can use a tensor nuclear norm regularization as the convex relaxation of the tensor rank. Tensor nuclear norm is the summation of M matrix nuclear norm

$$\mathcal{R}_{\text{low}}(\mathcal{W}) = \|\mathcal{W}\|_* = \frac{1}{M} \sum_{m=1}^M \|W_{(m)}\|_*, \quad (6)$$

where $\|W_{(m)}\|_*$ is the matrix nuclear norm for the m -th mode. This tensor nuclear norm is an extension of a matrix nuclear norm and is proven to automatically obtain a low-rank tensor both accurately and reliably. So our model uses the tensor nuclear norm to reduce model complexity.

4 Method

Model Overview We propose the Sparse and Low-Rank High-Order Tensor Regression (SLTR) method, which optimizes a tensor regression problem with sparse and low-rank regularizers. We extend a linear regression framework to fit the tensor data and multiple regularizers. Also, to speed up the optimization, we propose a fast and scalable algorithm that computes predictions for each mode in parallel. Fig. 1 gives a schematic of our model.

4.1 Optimization Problem: Multi-Regularized Tensor Regression with Fast Approximation

How to analyze the relationship between vector variables and responses in high-dimensional settings has been well studied in the linear regression literature. Among various methods, Elem-Ridge (Yang et al., 2014) is a novel estimation framework that enables fast optimization. Specifically, given variables $X \in \mathbb{R}^{N \times p}$ and responses $y \in \mathbb{R}^N$ of N observations, Elem-Ridge assumes $y = Xw + \gamma$ and solves

$$\widehat{w} = \arg \min_{w \in \mathbb{R}^p} \mathcal{R}(w) \quad \text{s.t.} \quad \mathcal{R}^* \left(w - \left(X^\top X + \varepsilon \mathbf{I} \right)^{-1} X^\top y \right) \leq \lambda. \quad (7)$$

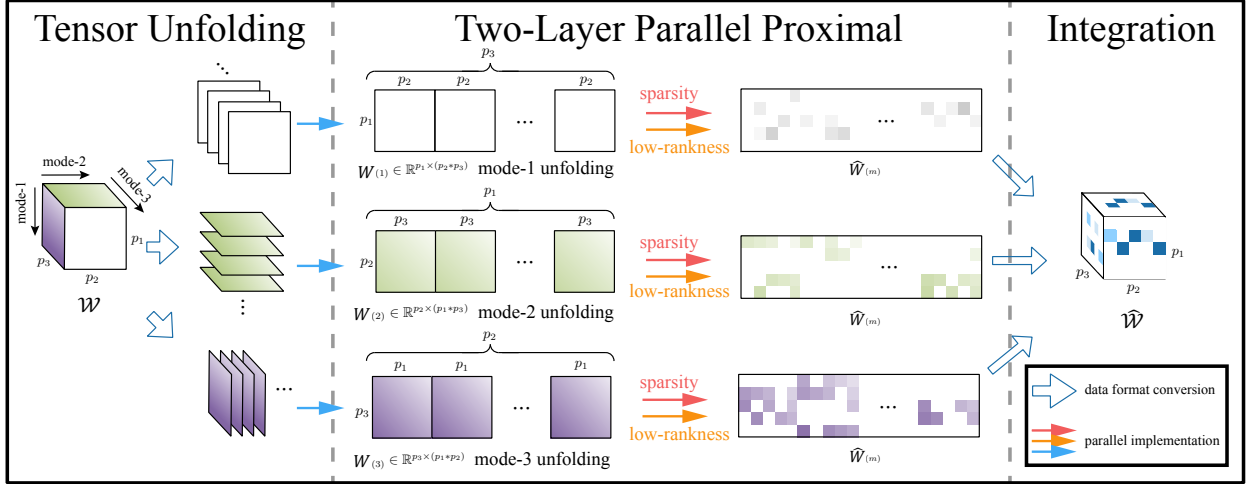


Figure 1: The basic idea of SLTR. We first unfold the tensor along each mode axis. Then for each mode, we parallelly estimate sparse and low-rank coefficients with proximal gradient descent. Finally, all mode estimations are integrated to obtain the final solution.

Here, \mathcal{R}^* is the dual norm of \mathcal{R} , \mathbf{I} is an identity matrix, and ε is a hyper-parameter dealing with the non-invertible sample covariance in high-dimensional cases. λ is another hyper-parameter setting the constraint bound.

Elem-Ridge inherits the primal-dual idea of the well-known Dantzig selector (Candes et al., 2007) that obtains structural properties by minimizing the norm \mathcal{R} while regressing the predictors y through the dual-norm \mathcal{R}^* . For example, if one requires sparsity, Elem-Ridge should use ℓ_1 norm as \mathcal{R} for variable selection and uses ℓ_∞ as the dual. The advantage of Elem-Ridge is it starts the optimization of coefficients w from an approximation $(X^\top X + \varepsilon \mathbf{I})^{-1} X^\top y$ instead of a random feasible point. The approximation is a Ridge estimator, denoting it is not too distinct from the optimal solution but only lacks demanded structural properties. Therefore, the optimization can converge in a few iterations. Moreover, because the approximation only computes once and can be easily accelerated with GPUs, Elem-Ridge significantly reduces the time cost.

In this paper, we derive a novel tensor regression method SLTR by extending Elem-Ridge to the tensor data and integrating multiple regularizers. We use the element-wise norm and tensor nuclear norm defined in Eq. (4) and Eq. (6) to obtain sparse and low-rank estimations. Concretely, given N samples of M -order tensor $\mathcal{X} \in \mathbb{R}^{N \times p_1 \times \dots \times p_M}$ and corresponding responses $y \in \mathbb{R}^N$, our SLTR aims to solve

$$\begin{aligned} \widehat{\mathcal{W}} &= \arg \min_{\mathcal{W}} \mathcal{R}_{\text{sparse}}(\mathcal{W}) + \mathcal{R}_{\text{low}}(\mathcal{W}) \\ \text{s.t. } \mathcal{R}_{\text{sparse}}^*(\mathcal{W} - \widetilde{\mathcal{W}}) &\leq \lambda_{\text{sparse}} \\ \mathcal{R}_{\text{low}}^*(\mathcal{W} - \widetilde{\mathcal{W}}) &\leq \lambda_{\text{low}} \end{aligned} \quad (8)$$

with the approximation and dual norms as

$$\begin{aligned} \widetilde{\mathcal{W}} &= \mathcal{T}_{\mathcal{P}} \left((X^\top X + \varepsilon \mathbf{I})^{-1} X^\top y \right) \\ \mathcal{R}_{\text{sparse}}^*(\mathcal{W} - \widetilde{\mathcal{W}}) &= \|\mathcal{W} - \widetilde{\mathcal{W}}\|_\infty \\ \mathcal{R}_{\text{low}}^*(\mathcal{W} - \widetilde{\mathcal{W}}) &= \|\mathcal{W} - \widetilde{\mathcal{W}}\|_2. \end{aligned} \quad (9)$$

We extend the approximation in Eq. (7) to tensors through unfolding-folding operations. The approximation $\widetilde{\mathcal{W}}$ is computed by first unfolding \mathcal{X} into matrix X through $X = \text{concat}(X_1, \dots, X_N) \in \mathbb{R}^{N \times \prod_m p_m}$ with each row $X_i = \text{vec}(\mathcal{X}_i) \in \mathbb{R}^{\prod_m p_m}$ a vectorization of the i -th observation. Then we use the folding operation $\mathcal{T}_{\mathcal{P}}(\cdot)$ to convert the Ridge estimator back to the tensor, given the size of each mode as $\mathcal{P} = \{p_1, p_2, \dots, p_M\}$. Because $\mathcal{R}_{\text{sparse}}$ is the

element-wise ℓ_1 norm, its dual is element-wise ℓ_∞ norm. Also, notice the tensor nuclear norm \mathcal{R}_{low} is a summation of the matrix nuclear norm, its dual can be easily extended from the matrix spectral norm³.

4.2 Optimization Solution: Two-Layer Parallel Proximal Algorithm

Based on the definition of element-wise ℓ_1 norm, we can write it as $\|\mathcal{W}\|_1 = \frac{1}{M} \sum_{m=1}^M \|W_{(m)}\|_1$, the average of element-wise ℓ_1 norm for each mode. This implies the ℓ_1 norm computation for each mode m is independent. Moreover, in Eq. (6), the tensor nuclear norm is also defined as the average of each mode's nuclear norm. Therefore, we can decompose Eq. (8) into M parallel sub-tasks

$$\begin{aligned} \widehat{W}_{(m)} &= \arg \min_{W_{(m)}} \|W_{(m)}\|_1 + \|W_{(m)}\|_* \\ \text{s.t.} \quad & \|W_{(m)} - \widetilde{W}_{(m)}\|_\infty \leq \lambda_{\text{sparse}} \\ & \|W_{(m)} - \widetilde{W}_{(m)}\|_2 \leq \lambda_{\text{low}}. \end{aligned} \quad (10)$$

After estimating $\widehat{W}_{(m)}$ for all modes $m = 1, \dots, M$, we integrate them into the final estimation

$$\widehat{\mathcal{W}} = \frac{1}{M} \sum_{m=1}^M \mathcal{T}_{\mathcal{P}} \left(\widehat{W}_{(m)} \right). \quad (11)$$

We solve each sub-task (Eq. (10)) through the parallel proximal algorithm Combettes and Pesquet (2011). We let $W \triangleq W_{(m)}$ for simplicity. Estimating $W_{(m)}$ is equivalent to

$$\arg \min_{W_1=W_2=W_3=W_4} f_1(W_1) + f_2(W_2) + f_3(W_3) + f_4(W_4) \quad (12)$$

by converting norms and corresponding constraints into

$$\begin{aligned} f_1(W) &= \|W\|_1 & f_2(W) &= \|W\|_* \\ f_3(W) &= \mathcal{I}_{\{\|W - \widetilde{W}_{(m)}\|_\infty \leq \lambda_{\text{sparse}}\}}(W) & f_4(W) &= \mathcal{I}_{\{\|W - \widetilde{W}_{(m)}\|_2 \leq \lambda_{\text{low}}\}}(W) \end{aligned} \quad (13)$$

where $\mathcal{I}_C(W)$ is an indicator function of set C as $\mathcal{I}_C(W) = 0$ if $W \in C$, otherwise $\mathcal{I}_C(W) = \infty$.

The parallel proximal algorithm solves Eq. (12) with proximal operators that compute convex approximations for non-differentiable functions like ℓ_1 norm and indication function. Here, we define proximal operators for Eq. (12). Specifically, for f_1 and f_3 , we have

$$\text{prox}_{f_1}(W; \lambda_{\text{sparse}}) = S_{\lambda_{\text{sparse}}}(W) \quad \text{with} \quad [S_{\lambda_{\text{sparse}}}(W)]_{ij} = \text{sign}(W_{ij}) \max\{|W_{ij}| - \lambda_{\text{sparse}}, 0\} \quad (14)$$

and

$$\text{prox}_{f_3}(W; \lambda_{\text{sparse}}) = \begin{cases} \widetilde{W}_{ij}, & |W_{ij} - \widetilde{W}_{ij}| \leq \lambda_{\text{sparse}} \\ \widetilde{W}_{ij} + \lambda_{\text{sparse}}, & W_{ij} - \widetilde{W}_{ij} > \lambda_{\text{sparse}} \\ \widetilde{W}_{ij} - \lambda_{\text{sparse}}, & W_{ij} - \widetilde{W}_{ij} < -\lambda_{\text{sparse}} \end{cases}. \quad (15)$$

The other two nuclear-norm-relevant proximal operators are computed based on singular value decomposition (SVD). For a matrix W , SVD decomposes it into $W = U\Sigma V^\top$ in which Σ is a diagonal matrix with singular values on its diagonal and U, V are left and right singular vectors correspondingly. Based on this, we have

$$\text{prox}_{f_2}(W; \lambda_{\text{low}}) = US_{\lambda_{\text{low}}}(\Sigma)V^\top \quad \text{with} \quad [S_{\lambda_{\text{low}}}(\Sigma)]_{ii} = \text{sign}(\Sigma_{ii}) \max\{|\Sigma_{ii}| - \lambda_{\text{low}}, 0\} \quad (16)$$

and

$$\text{prox}_{f_4}(W; \lambda_{\text{low}}) = \begin{cases} \widetilde{W}, & \sigma_{\max}(W) \leq \lambda_{\text{low}} \\ US_{\lambda_{\text{low}}}(\Sigma)V^\top + \widetilde{W}, & \sigma_{\max}(W) > \lambda_{\text{low}} \end{cases} \quad (17)$$

where $\sigma_{\max}(W)$ represents the maximum eigenvalue of W . Given these proximal operators, our optimization solution is summarized in Algorithm 1. Notice the sub-task optimizations are parallel, and the computation of four proximal operators within each sub-task is also parallel. Hence, our algorithm obtains the solution in the manner of two-layer parallelism.

³We are not directly applying these norm functions on tensor data. Notice that both ℓ_1 norm and tensor nuclear norm can be easily reformulated into the combination of multiple matrix norms, we can straightforwardly define them and corresponding dual norms on tensors. See Eq. (10)

Algorithm 1 Parallel Proximal Based Algorithm for SLTR

- 1: **Input:** $\mathcal{X} \in \mathbb{R}^{N \times p_1 \times p_2 \times \dots \times p_M}$, $y \in \mathbb{R}^N$, initial approximation $\widetilde{\mathcal{W}}$, the maximum number of iterations T , learning rate $\rho \in [0, 2]$, and tuning parameters $\mathbf{c} = (\lambda_{\text{sparse}}, \lambda_{\text{sparse}}, \lambda_{\text{low}}, \lambda_{\text{low}})$.
- 2: **for** $m = 1$ to M **paralelly do**
- 3: **Initialize** $W_{(m)} = W_{(m)1}^1 = W_{(m)2}^1 = W_{(m)3}^1 = W_{(m)4}^1 = \widetilde{W}_{(m)}$
- 4: **for** $t = 1$ to T **do**
- 5: **for** $i = 1, 2, 3, 4$ **paralelly do**
- 6: $a_i^t = \text{prox}_{f_i} \left(W_{(m)i}^t ; 4\mathbf{c}_i \right)$
- 7: **end for**
- 8: $a^t = \frac{1}{4} \sum_{i=1}^4 a_i^t$
- 9: **for** $i = 1, 2, 3, 4$ **do**
- 10: $W_{(m)i}^{t+1} = W_{(m)i}^t + \rho(2a^t - W_{(m)} - a_i^t)$
- 11: **end for**
- 12: $W_{(m)} = W_{(m)} + \rho(a^t - W_{(m)})$
- 13: **end for**
- 14: $\widehat{\mathcal{W}}_m = \mathcal{T}_{\mathcal{P}} \left(W_{(m)} \right)$
- 15: **end for**
- 16: **Output:** $\widehat{\mathcal{W}} = \frac{1}{M} \sum_{m=1}^M \widehat{\mathcal{W}}_m$.

4.3 Running Time Complexity

First of all, the initial approximation $\widetilde{\mathcal{W}}$ is only computed once and reused in the algorithm. Because computing $\widetilde{\mathcal{W}}$ requires only simple operations such as matrix multiplication and matrix inversion, this part can be easily speeded up with multi-thread computing and rapidly obtained as the pre-condition of our algorithm. In Sec. 7, we show that the individual pre-condition calculation of SLTR enables more rapid estimation with hyper-parameter tuning. Given $\widetilde{\mathcal{W}}$, totally M sub-tasks are solved simultaneously using parallel proximal-based algorithm Algorithm 1. Within each sub-task, the computation is dominated by the SVD procedure with $O(p_m (\prod_{k \neq m} p_k)^2)$ time complexity. So overall, by virtue of our two-layer parallel solution, the computational bottleneck of solving SLTR can be considered as only $O(\max_m \{p_m (\prod_{k \neq m} p_k)^2\})$.

5 Theoretical Analysis

We now prove the convergence rate of SLTR. We follow the proof of Yang et al. (2014) and assume the following:

(C1: sparse) The optimal coefficient \mathcal{W}^* has exactly k non-zero elements.

(C2: low-rank) The optimal coefficient \mathcal{W}^* is an R -rank tensor, where $R = \max_{\mathcal{A} \in \mathbb{R}^{p_1 \times \dots \times p_M}} (r_{\perp}(\mathcal{A}))$ and $r_{\perp}(\mathcal{A})$ denotes the orthogonal rank of \mathcal{A} . The orthogonal rank is the smallest number that satisfies $\mathcal{A} = \sum_{r=1}^{r_{\perp}(\mathcal{A})} \mathcal{U}_r$ with $\langle \mathcal{U}_{r_1}, \mathcal{U}_{r_2} \rangle = 0$, $r_1 \neq r_2$ for $1 \leq r_1 \leq r_{\perp}(\mathcal{A})$, $1 \leq r_2 \leq r_{\perp}(\mathcal{A})$.

Theorem 1. Suppose we solve Eq. (8) with proper controlling parameters λ_{sparse} and λ_{low} . Then, the estimation satisfies the error bound

$$\|\widehat{\mathcal{W}} - \mathcal{W}^*\|_F \leq 4\sqrt{2} \left(\lambda_{\text{sparse}} \sqrt{\prod_{m=1}^M p_m} + \lambda_{\text{low}} \sqrt{R} \right). \quad (18)$$

Corollary 5.1. In the three-order tensor case where $\mathcal{W} \in \mathbb{R}^{p_1 \times p_2 \times p_3}$, the estimation of Eq. (8) satisfies the error bound

$$\|\widehat{\mathcal{W}} - \mathcal{W}^*\|_F \leq 4\sqrt{2} \left(\lambda_{\text{sparse}} \sqrt{\prod_{m=1}^M p_m} + \lambda_{\text{low}} \max_{k=1,2,3} \{R_k'\} \right), \quad (19)$$

where $r_m = \text{rank}(\mathcal{W}_{(m)})$ denotes the rank of the unfolded matrix. $R'_1 = \sqrt{r_1 \min\{r_2, r_3\}}$, $R'_2 = \sqrt{r_2 \min\{r_1, r_3\}}$, and $R'_3 = \sqrt{r_3 \min\{r_1, r_2\}}$.

All proofs are provided in the appendix.

6 Related Works

Some tensor regression methods (He et al., 2018; Zhou et al., 2013; Guo et al., 2011) have been proposed based on CP decomposition. Generally, these methods aim at inferring decomposed components to approximate low-rank estimations. For example, Zhou et al. (2013) proposed Generalized Linear Tensor Regression Model using the generalized linear model (GLM). In addition, He et al. (2018) recently proposed Stagewise Unit-Rank Tensor Factorization (SURF) exploiting the divide-and-conquer strategy where the sub-task has a similar formulation of Elastic Net (Zou and Hastie, 2005). Almost all the CP-decomposition-based methods require prior knowledge of the CP-rank R . However, we always have little information about it in real-world applications. Even if we can use techniques, such as cross-validation, to select R from a wide range, choosing the R value becomes complicated and computationally expensive for large-scale data. Moreover, the larger R is, the more computational time is required for these methods. Therefore, these methods are not suitable for real-world applications.

In another line of work, structural constraints are directly applied to the coefficient tensor rather than its decomposed components in order to avoid expensive decomposition. For instance, in Regularized multilinear regression and selection (Remurs) (Song and Lu, 2017), the tensor nuclear norm and ℓ_1 norm are used. However, these methods are computationally expensive because non-differential regularizers exist in their objective function and the lack of parallelism. We compare our SLTR with state-of-the-art tensor regression models in Table 1. SLTR outperforms other methods on model abilities and computational time complexity.

Table 1: Comparison between SLTR and other tensor regression models. T denotes the number of iterations for iterative method, N is the number of samples, M is the number of modes, and R is the CP-rank. $\mathbf{P} = \prod_{m=1}^M p_m$ and $\mathbf{P}_{\setminus m} = \prod_{k \neq m}^M p_k$. T is the number of SURF iterations. We compare their computational bottlenecks and properties.

	SLTR	Remurs	GLTRM	orTRR	SURF	LR
Comp. Bottleneck	$O(\max_m \{p_m \cdot \mathbf{P}_{\setminus m}^2\})$	$O(\sum_{m=1}^M \{p_m \cdot \mathbf{P}_{\setminus m}^2\})$	$O(R \sum_{m=1}^M p_m^3)$	$O(M \cdot \mathbf{P}^3)$	$O(TN \cdot \sum_{m=1}^M \mathbf{P}_{\setminus m})$	$O(N \cdot \mathbf{P}^2)$
Auto-Explored Rank	✓	✓	×	✓	×	×
Sufficient Sparsity	✓	✓	✓	×	✓	✓
Structure Reserved	✓	✓	✓	✓	✓	×

7 Experiment

Baselines We compare our SLTR with four previously proposed methods, representing different groups of tensor regression methods, including (1) Linear regression models, specifically, Lasso and Elastic Net (with trade-off ratio between ℓ_1 and ℓ_2 norm being 0.5)⁴, (2) Remurs (Song and Lu, 2017), and (3) SURF (He et al., 2018). All the methods are implemented in MATLAB.

Evaluation metrics For experiments on simulated datasets (Section 7.1), we report the computational time cost (in seconds) and prediction mean squared error (MSE) for all the methods. For experiments on the video action recognition dataset (Section 7.2), we report the computational time cost (in seconds) and area under receiver operating characteristic (AUROC) for each pair of action labels.

Hyper-parameter tuning Tuning hyper-parameters of all the methods are selected through cross-validation procedures which take the average performance on validation datasets as the selecting criteria. We tune hyper-parameters from a wide range of values to ensure each method achieves its best performance. The ranges of hyper-parameters are listed in the appendix.

Other setups We set the maximal number of iterations to be 1000 for all the methods and let them terminate when the iteration update $\frac{\|\mathcal{W}^{t+1} - \mathcal{W}^t\|_F}{\|\mathcal{W}^t\|_F} \leq 10^{-4}$. We run every single experiment ten times and report the average value of metrics over these ten trials.

⁴Here, we employ Lasso and Elastic Net on the vectorized data.

7.1 Simulated Data: Tensor Regression

We first test our model on simulated datasets. The dataset is generated through the following steps:

- **(Step 1)** Specify the optimal coefficient tensor $\mathcal{W}^* \in \mathbb{R}^{p_1 \times p_2 \times \dots \times p_M}$ and N samples $\mathcal{X} \in \mathbb{R}^{N \times p_1 \times p_2 \times \dots \times p_M}$ with each element drawn from the normal distribution $\mathcal{N}(0, 1)$.
- **(Step 2)** Randomly set $s\%$ elements of \mathcal{W} to be 0.
- **(Step 3)** Compute N responses $y \in \mathbb{R}^N$ through $y_i = \langle \mathcal{W}^*, \mathcal{X}_i \rangle + 0.1\gamma_i$, where the noise ε_i is generated from the normal distribution $\mathcal{N}(0, 0.1)$.

We simulate 3D and 4D datasets with different shapes by fixing the sparsity level $s\% = 80\%$. Because the SURF implementation does not apply to 4D data, we omit it in 4D data experiments. This also indicates its limitations in broader applications.

We report MSE values of estimation on high-dimensional simulated datasets in Table 2. The number of samples is determined through $N = 8\% \cdot \prod_{m=1}^M p_m$ for each dataset in order to construct high-dimensional settings. The result indicates that SLTR has the best estimation in most cases, while its estimations are only slightly worse than the best in other cases. The MSE values of tensor regression models are significantly lower than those of linear regression models, indicating that linear regression indeed discards the structural information of tensors. In addition, we investigate how estimations improve if we use more samples. Specifically, we simulate 3D datasets with the shape of $20 \times 20 \times 5$ and vary the number of samples N from 50 to 400. Table 3 shows that SLTR obtains the best estimation under almost all conditions. Moreover, the MSE decreases when more samples are provided, as we expect.

Table 2: MSE on simulated datasets of different variable sizes. The bold number denotes the best method and the underlined value represents the second best result.

size	SLTR	Remurs	SURF	Lasso	Elastic Net
<i>3D Data – 8% samples</i>					
$30 \times 30 \times 5$	0.9186	<u>0.9190</u>	0.9289	1.9381	1.9377
$35 \times 35 \times 5$	0.9336	<u>0.9370</u>	0.9527	2.0147	2.0147
$40 \times 40 \times 5$	<u>0.9073</u>	0.9072	1.0006	2.1059	2.1065
<i>4D Data – 8% samples</i>					
$20 \times 20 \times 10 \times 5$	0.9150	<u>0.9177</u>		2.1388	2.1373
$25 \times 25 \times 10 \times 5$	0.9071	<u>0.9101</u>	N/A	1.9696	1.9696
$30 \times 30 \times 10 \times 5$	0.9110	<u>0.9123</u>		1.9754	1.9745

Table 3: MSE on simulated datasets of different numbers of samples. The number of samples varies from 50 to 400. The bold number denotes the best method and the underlined value represents the second best result.

sample numbers (N)	SLTR	Remurs	SURF	Lasso	Elastic Net
50	1.6123	<u>1.6198</u>	1.6439	4.5083	4.5759
100	1.0798	<u>1.0946</u>	1.7101	1.6433	1.6433
150	<u>0.9295</u>	0.9190	0.9953	1.6777	1.6502
200	0.8351	<u>0.8469</u>	0.8376	1.9072	0.8376
250	0.7130	<u>0.7267</u>	<u>0.7199</u>	1.3757	1.3708
300	0.7282	<u>0.7325</u>	0.7524	1.7316	1.6938
350	0.6275	<u>0.6275</u>	0.6379	1.3207	1.2804
400	0.5954	<u>0.5969</u>	0.5975	1.1487	1.1450

The benefit of our SLTR is it uses a fast approximation to speed up computations. Especially in hyper-parameter tuning, SLTR only needs to compute the approximation $\widetilde{\mathcal{W}}$ once (for one ϵ value) when changing the value of controlling hyper-parameters. Since hyper-parameter tuning is a necessary procedure in model selection, fast approximation enables SLTR to obtain the best solution with much fewer time costs than previous methods. To validate this, we record the time cost of hyper-parameter tuning for SLTR and Remurs. They have two common hyper-parameters λ_{sparse} and λ_{low} controlling the degree of sparsity and low-rankness. We tune each of them from seven values $\{0.005, 0.01, 0.05, 0.1, 0.5, 1, 5\}$. Moreover, SLTR has an extra hyper-parameter ϵ for approximation computation, which we tune from three values $\{0.1, 0.2, 0.3\}$. So SLTR and Remurs use 147 and 49 groups of hyper-parameters, respectively. We record the time of the method running with each hyper-parameter group and report the total time cost on all groups. Table 4 indicates that SLTR is faster than Remurs by orders of magnitude, and the speedup becomes increasingly evident as the size of the data increases. Therefore, even though our SLTR has one more hyper-parameter than Remurs, its time cost is largely reduced by virtue of the fast and one-time approximation calculation.

Table 4: Time costs (in seconds) of hyper-parameter tuning. The “speedup” is computed by dividing Remurs cost by SLTR cost.

size	SLTR	Remurs	speedup
<i>3D Data – 8% samples</i>			
$30 \times 30 \times 5$	16.793568	510.050226	30.37 ×
$30 \times 30 \times 5$	20.212862	602.292492	29.80 ×
$30 \times 30 \times 5$	6.509343	684.737448	105.20 ×
<i>4D Data – 8% samples</i>			
$20 \times 20 \times 10 \times 5$	10.975796	1474.090235	134.30 ×
$25 \times 25 \times 10 \times 5$	16.936689	3060.085998	180.67 ×
$30 \times 30 \times 10 \times 5$	23.276677	3394.478247	145.83 ×

Overall, experiments on simulated datasets validate that SLTR predict better estimations with much less time costs.

7.2 Real-World Case: Video Action Recognition

We then evaluate our method on the UCF101 (Soomro et al., 2012), a video action recognition dataset. It collects 13320 videos of 101 action categories from YouTube. Each video has a different time length, ranging from less than 2 seconds to longer than 10 seconds, with each frame having a resolution of $320 \text{ pixels} \times 240 \text{ pixels}$. We focus on binary classification tasks and choose three pairs of categories: “ApplyEyeMakeup” vs. “ApplyLipstick”, “BaseballPitch” vs. “Basketball”, and “BodyWeightSquats” vs. “Bowling”. We uniformly extract 15 frames with a fixed interval from each video and transform them into the grey scale. For each frame, we resize it into $32 \text{ pixels} \times 24 \text{ pixels}$ by averaging neighboring pixels. So each sample is a $15 \times 32 \times 24$ tensor. For each pair of categories, we select 80% of samples for training and the other 20% for testing. We use AUROC scores to evaluate the classification performance.

Table 5 shows that SLTR reaches nearly the best AUROC scores. Only the AUROC scores of Remurs are comparable to SLTR. In the first pair of labels, SLTR has a slightly smaller AUROC value and performs much better than SURF and two linear models. In the other two cases, our SLTR has the most accurate estimations among all methods. Furthermore, we compare the hyper-parameter tuning time cost of SLTR (with 80 groups of hyper-parameters) and Remurs (with 49 groups of hyper-parameters). Table 6 shows that SLTR has a significant time advantage over Remurs. This implies that SLTR has good estimations with lesser time costs.

Table 5: AUROC values on the UCF101 dataset. The bold number denotes the best AUROC value, while underlined number highlights the second best.

Label Pair	SLTR	Remurs	SURF	Lasso	Elastic Net
“ApplyEyeMakeup” & “ApplyLipstick”	0.931953	0.945266	0.64053	0.88006	0.887556
“BaseballPitch” & “Basketball”	0.995074	0.995074	0.78695	0.964194	0.965473
“BodyWeightSquats” & “Bowling”	0.97756	<u>0.946704</u>	0.32258	0.919753	0.930556

Table 6: Hyper-parameter tuning time cost (in seconds) on the UCF101 dataset.

Lable pair	SLTR	Remurs	speedup
“ApplyEyeMakeup” & “ApplyLipstick”	6.889112525	692.231181	100.48 ×
“BaseballPitch” & “Basketball”	6.865089138	678.267903	98.80 ×
“BodyWeightSquats” & “Bowling”	6.638173225	701.628673	105.67 ×

Lastly, we visualize estimated coefficients in Fig. 2. The heatmap shows the superior interpretability of SLTR. For example, in a video of the “ApplyEyeMakeup” class (first row in Fig. 2), the focus of SLTR (i.e., high estimated weights) is mainly on the eyes. Remurs shows similar interpretations while SLTR estimations are more sparse. SURF estimations are all close to zeros, which explains its terrible AUROC value. Linear methods only focus on a few spots that cannot help with interpretations. Experiments on this classification task indicate that SLTR can give accurate and interpretable solutions with much fewer time costs.



Figure 2: Example heatmaps of estimated coefficients on one frame of four videos.

8 Conclusion

This paper proposes a fast and scalable tensor regression method that directly imposes structural constraints on the tensor variables. A two-layer parallel solution is also proposed to solve the problem effectively. The benefit of our model is that fast approximation vastly reduces computational time costs, especially in hyper-parameter tuning.

The work may attract the interest of researchers from various fields when analyzing relationships for tensor data. The targeted areas include neuroscience and bioinformatics. For example, in neuroscience, the model can be applied to high-dimensional fMRI data to analyze the relationship between brain activities and disease symptoms.

In future work, we will explore variations of our method on data with modes denoting special relationships. For example, the *time* mode of video data should have temporal dependencies. Adding extra constraints over such a relationship will increase the performance of SLTR in specific video analysis applications. Moreover, we will extend our model to more general cases regarding the tensor-on-vector or tensor-on-tensor regression.

References

- Ahmed, T., Raja, H., and Bajwa, W. U. (2020). Tensor regression using low-rank and sparse tucker decompositions. *SIAM Journal on Mathematics of Data Science*, 2(4):944–966.
- Bhargava, P., Phan, T., Zhou, J., and Lee, J. (2015). Who, what, when, and where: Multi-dimensional collaborative recommendations using tensor factorization on sparse user-generated data. In *Proceedings of the 24th international conference on world wide web*, pages 130–140. International World Wide Web Conferences Steering Committee.
- Candes, E., Tao, T., et al. (2007). The dantzig selector: Statistical estimation when p is much larger than n . *The annals of Statistics*, 35(6):2313–2351.
- Cichocki, A., Lee, N., Oseledets, I., Phan, A.-H., Zhao, Q., Mandic, D. P., et al. (2016). Tensor networks for dimensionality reduction and large-scale optimization: Part 1 low-rank tensor decompositions. *Foundations and Trends® in Machine Learning*, 9(4-5):249–429.
- Combettes, P. L. and Pesquet, J.-C. (2011). Proximal splitting methods in signal processing. In *Fixed-point algorithms for inverse problems in science and engineering*, pages 185–212. Springer.
- Guo, W., Kotsia, I., and Patras, I. (2011). Tensor learning for regression. *IEEE Transactions on Image Processing*, 21(2):816–827.
- He, L., Chen, K., Xu, W., Zhou, J., and Wang, F. (2018). Boosted sparse and low-rank tensor regression. In *Advances in Neural Information Processing Systems*, pages 1009–1018.
- Heinze, G., Wallisch, C., and Dunkler, D. (2018). Variable selection—a review and recommendations for the practicing statistician. *Biometrical journal*, 60(3):431–449.

- Ji, Y., Wang, Q., Li, X., and Liu, J. (2019). A survey on tensor techniques and applications in machine learning. *IEEE Access*, 7:162950–162990.
- Li, N., Kindermann, S., and Navasca, C. (2013). Some convergence results on the regularized alternating least-squares method for tensor decomposition. *Linear Algebra and its Applications*, 438(2):796–812.
- Li, W., Lou, J., Zhou, S., and Lu, H. (2019). Sturm: Sparse tubal-regularized multilinear regression for fmri. In *International Workshop on Machine Learning in Medical Imaging*, pages 256–264. Springer.
- Lim, L.-H. and Hillar, C. (2009). Most tensor problems are np hard. *University of California, Berkeley*.
- Liu, J., Musialski, P., Wonka, P., and Ye, J. (2012). Tensor completion for estimating missing values in visual data. *IEEE transactions on pattern analysis and machine intelligence*, 35(1):208–220.
- Lui, Y. M. (2012). A least squares regression framework on manifolds and its application to gesture recognition. In *2012 IEEE Computer Society Conference on Computer Vision and Pattern Recognition Workshops*, pages 13–18. IEEE.
- Mitchell, T. M., Shinkareva, S. V., Carlson, A., Chang, K.-M., Malave, V. L., Mason, R. A., and Just, M. A. (2008). Predicting human brain activity associated with the meanings of nouns. *science*, 320(5880):1191–1195.
- Noroozi, A. and Rezghi, M. (2020). A tensor-based framework for rs-fmri classification and functional connectivity construction. *Frontiers in neuroinformatics*, 14:581897.
- Rabanser, S., Shchur, O., and Günnemann, S. (2017). Introduction to tensor decompositions and their applications in machine learning. *arXiv preprint arXiv:1711.10781*.
- Sharma, L. and Gera, A. (2013). A survey of recommendation system: Research challenges. *International Journal of Engineering Trends and Technology (IJETT)*, 4(5):1989–1992.
- Shitov, Y. (2016). How hard is the tensor rank? *arXiv preprint arXiv:1611.01559*.
- Song, X. and Lu, H. (2017). Multilinear regression for embedded feature selection with application to fmri analysis. In *Thirty-First AAAI Conference on Artificial Intelligence*.
- Soomro, K., Zamir, A. R., and Shah, M. (2012). Ucf101: A dataset of 101 human actions classes from videos in the wild.
- Tomioka, R., Hayashi, K., and Kashima, H. (2010). Estimation of low-rank tensors via convex optimization. *arXiv preprint arXiv:1010.0789*.
- Tucker, L. R. (1966). Some mathematical notes on three-mode factor analysis. *Psychometrika*, 31(3):279–311.
- Wu, X. and Lai, J. (2010). Tensor-based projection using ridge regression and its application to action classification. *IET image processing*, 4(6):486–493.
- Yang, E., Lozano, A., and Ravikumar, P. (2014). Elementary estimators for high-dimensional linear regression. In *International Conference on Machine Learning*, pages 388–396.
- Yang, Y., Krompass, D., and Tresp, V. (2017). Tensor-train recurrent neural networks for video classification. In *International Conference on Machine Learning*, pages 3891–3900. PMLR.
- Zhou, H., Li, L., and Zhu, H. (2013). Tensor regression with applications in neuroimaging data analysis. *Journal of the American Statistical Association*, 108(502):540–552.
- Zhu, D., Zhang, T., Jiang, X., Hu, X., Chen, H., Yang, N., Lv, J., Han, J., Guo, L., and Liu, T. (2014). Fusing dti and fmri data: a survey of methods and applications. *NeuroImage*, 102:184–191.
- Zou, H. and Hastie, T. (2005). Regularization and variable selection via the elastic net. *Journal of the royal statistical society: series B (statistical methodology)*, 67(2):301–320.